Published in final edited form as:
Neuron. 2012 August 23; 75(4): 618–632. doi:10.1016/j.neuron.2012.06.026.

Tau promotes neurodegeneration via DRP1 mislocalization in vivo

Brian DuBoff[1], **Jürgen Götz**[2], and **Mel B. Feany**[1,*]

[1]Department of Pathology, Brigham and Women's Hospital, Harvard Medical School, Boston, MA 02115, USA

[2]Centre for Ageing Dementia Research, Queensland Brain Institute, The University of Queensland, St Lucia Campus, QLD 4072, Australia

Summary

Mitochondrial abnormalities have been documented in Alzheimer's disease and related neurodegenerative disorders, but the causal relationship between mitochondrial changes and neurodegeneration, as well as the specific mechanisms promoting mitochondrial dysfunction, are not clear. Here we find that expression of human tau results in elongation of mitochondria in both *Drosophila* and mouse neurons. Elongation is accompanied by mitochondrial dysfunction and cell cycle-mediated cell death, which can be rescued in vivo by genetically restoring the proper balance of mitochondrial fission and fusion. We have previously demonstrated that stabilization of actin by tau is critical for neurotoxicity of the protein. Here we demonstrate a conserved role for actin and myosin in regulating mitochondrial fission, and show that excess actin stabilization inhibits association of the fission protein DRP1 with mitochondria leading to mitochondrial elongation and subsequent neurotoxicity. Our results thus identify actin-mediated disruption of mitochondrial dynamics as a direct mechanism of tau toxicity in neurons in vivo.

Introduction

Alzheimer's disease (AD) is the most common neurodegenerative disorder, affecting approximately 10% of people over the age of 70 (Plassman et al., 2007). AD is characterized histopathologically by deposition of Abeta peptides in extracellular amyloid plaques and by aggregation of hyperphosphorylated species of the microtubule- associated protein tau into neurofibrillary aggregates in the cytoplasm of neurons. Experimental evidence supports the amyloid cascade hypothesis in which Abeta peptides act upstream of tau to mediate neurodegeneration in AD (Hardy and Selkoe, 2002; Ittner and Gotz, 2010). Importantly, dominant, highly penetrant mutations in the *tau* (*MAPT*) gene cause the familial neurodegenerative disease frontotemporal dementia with parkinsonism linked to chromosome 17 (FTDP-17), demonstrating an unequivocal role for tau in mediating neurodegeneration in patients (Hutton et al., 1998; Poorkaj et al.; 1998, Spillantini et al., 1998). AD and related disorders characterized by abnormal deposition of tau are collectively termed "tauopathies."

*Correspondence: mel_feany@hms.harvard.edu.

Despite the substantial evidence linking tau to neurodegeneration, the mechanisms downstream of tau that promote dysfunction and death of neurons are still incompletely understood. A potential role for abnormalities of mitochondrial structure and function in tauopathies has been attractive for a number of reasons. First, mitochondria are critical regulators of a variety of important cellular processes, including ATP production and metabolism of reactive oxygen species. Second, abnormalities in mitochondrial function have been strongly linked to aging, the most important risk factor for AD (Bratic and Trifunovic, 2010). In addition, mitochondrial morphological defects have been observed in patients with AD (Hirai et al., 2001). A number of reports have suggested dysfunction of mitochondria in tauopathy patients and disease models, based on reduced levels of mitochondrial metabolic proteins including pyruvate dehydrogenase (Perry et al., 1980), ATP synthase (David et al., 2005), and Complex I (Rhein et al., 2009). While these data taken together argue convincingly for mitochondrial abnormalities in AD and related tauopathies, the precise nature of the fundamental defects and the causal role those defects play in disease pathogenesis has been unclear.

In the current study we demonstrate increased length of mitochondria in animal models of tauopathy. Mitochondrial morphology is regulated by reciprocal membrane fission and fusion, termed mitochondrial dynamics. In mammalian cells, outer mitochondrial membrane fusion is induced by mitofusin-1 and -2 (MFN1 and MFN2), and inner membrane fusion by OPA1(Chen et al., 2003; Cipolat et al., 2004). Mitochondrial fission is dependent on the dynamin-related GTPase DRP1, which is primarily cytoplasmic with a smaller fraction localizing to the outer mitochondrial membrane (Smirnova et al., 2001). Translocation of DRP1 from cytoplasm to mitochondria appears to play a critical role in the regulation of fission (Frank et al., 2001). Rare inherited neurological disorders reveal the importance of normal mitochondrial dynamics in postmitotic neurons. Charcot-Marie-Tooth disease type 2A (CMT2A), a progressive sensory and motor axonopathy, is caused by mutations in *MFN2* (Zuchner et al., 2004). Similarly, mutations in *OPA1* underlie the autosomal dominant optic atrophy syndrome, a degeneration that targets retinal ganglion cells (Alexander et al., 2000; Delettre et al., 2000). Additionally, a severe neurodevelopmental syndrome has been reported in a patient with a dominant negative mutation in *DRP1* (Waterham et al., 2007). However, the contribution of abnormal mitochondrial dynamics to the pathogenesis of common neurodegenerative diseases, like AD, has been less clear.

To take a genetic approach to the mechanisms underlying neurodegeneration in AD and related tauopathies, we have developed a *Drosophila* model that recapitulates a number of salient features of the human disorders. Expression of wild type and mutant versions of human tau in flies results in aberrant phosphorylation and aggregation of tau, progressive neurodegeneration, and early death (Wittmann et al., 2001; Jackson et al., 2002; Nishimura et al., 2004; Khurana et al., 2010). We have subsequently defined a number of mechanisms that are critical for neurodegeneration in our tauopathy model. These mechanisms are implicated in human AD and related tauopathies, as well. Neurotoxicity in our system requires phosphorylation of tau as an early event (Steinhilb et al., 2007a; Steinhilb et al., 2007b; Iijima-Ando et al., 2010). Tau then directly binds to and stabilizes actin (Fulga et al., 2006). However, the mechanism by which actin stabilization promotes downstream mediators of neurotoxicity has been unclear. The molecular machinery that drives mitochondrial dynamics is well conserved in *Drosophila* (Verstreken et al., 2005; Hwa et al., 2002). We now identify actin-mediated DRP1 mislocalization as a critical effector of tau neurotoxicity in postmitotic neurons and further show that DRP1 localization to mitochondria requires the actin-based motor protein myosin II.

Results

Tau expression promotes mitochondrial elongation in neurons

Our *Drosophila* model of tauopathy is based on expression of either wild type or FTDP-17 linked mutant forms of tau in neurons using the UAS/GAL4 bipartite expression system (Brand and Perrimon, 1993) and a panneuronal driver (*elav-GAL4*). In these studies we predominantly express human tau carrying the R406W mutation, which, unless otherwise noted, we will refer to as "tau" for simplicity. We have previously found that the enhanced toxicity observed with expression of R406W mutant tau facilitates examination of neurodegeneration in the aging brain, with good conservation of mechanisms underlying neurotoxicity between mutant and wild type forms of human tau (Khurana et al., 2006; Fulga et al., 2006; Dias-Santagata et al., 2007; Khurana et al., 2010; Loewen and Feany, 2010). To examine mitochondrial morphology in our model we coexpressed tau with mitochondrially-localized GFP (mitoGFP) in neurons of the adult brain. Visualizing the neuronally-expressed and mitochondrially-directed GFP reveals normal round to tubular mitochondria in control neurons (Fig. 1A, control, arrowheads). In contrast, mitochondria in the neurons of brains from flies expressing tau are markedly elongated (Fig. 1A, tau, arrowheads). Quantification shows that in tau-expressing neurons mitochondrial length is, on average, greater than twice that of control (Fig. 1A, graph). Consistent with a causative role for altered mitochondrial dynamics in mediating tau neurotoxicity, mitochondrial elongation precedes cell death and increases with age (Fig. S1A,E). Mitochondrial elongation also correlates with in vivo toxicity of different forms of tau. Expression of tau^{R406W} induces greater mitochondrial elongation compared to expression of wild type human tau (tau^{WT}) expressed at the same levels, consistent with enhanced toxicity of tau^{R406W} compared to tau^{WT} (Wittmann et al., 2001; Khurana et al., 2006). Even greater elongation is triggered by expression of a more toxic, pseudohyperphosphorylated form of tau (tau^{E14}, Fig. S1B) (Dias-Santagata et al., 2007; Loewen and Feany, 2010), suggesting that mitochondrial elongation is downstream of tau phosphorylation.

Since a significant body of evidence links abnormalities of axonal transport to tauopathy pathogenesis (Ebneth et al., 1998; Dixit et al., 2008; Kopeikina et al., 2011; Ittner et al., 2009), we wondered if elongation of mitochondria in tau transgenic animals might be a secondary effect related to a defect in transport of mitochondria out of the cell body, rather than a primary abnormality. We thus evaluated mitochondrial length following inhibition of axonal transport of mitochondria. The miro and milton proteins are essential for association of mitochondria with the motor protein kinesin, which facilitates their microtubule-based transport (Glater et al., 2006). Consistent with a role for miro in mitochondrial trafficking, transgenic RNAi-mediated reduction of miro increases the mitochondrial content of the neuronal cell bodies. However, mitochondria in miro knockdown neurons are not elongated (Fig. 1A, miro RNAi, arrowheads). Similarly, in clones homozygous for $milton^{92}$, a null mutation (Glater et al., 2006), mitochondria are increased in neuronal soma, but are unchanged in length (Fig. S1A). Further, reduction of miro function does not alter mitochondrial morphology in the presence of transgenic tau, but is instead associated with increased numbers of both normal and elongated mitochondria in the neuronal cell bodies, as well as enhancement of tau neurotoxicity (Fig. S1D,E). Thus, elongation of mitochondria in tau transgenic animals does not appear to be a secondary effect of axonal transport defects.

We next determined if tau expression can alter mitochondrial morphology in vertebrate neurons. We used a murine model of tauopathy, rTg4510, in which human tau carrying the FTDP-17 linked P301L mutation is expressed using the CaMKIIα promoter (Ramsden et al., 2005; Santacruz et al., 2005). To visualize mitochondria in histologic sections from these transgenic mice we performed immunofluorescent staining for ATP synthase. We observe

round to modestly tubular mitochondria in hippocampal pyramidal neurons of control mice (Fig. 1B, control, arrowheads). In contrast, mitochondria in hippocampal pyramidal neurons, a vulnerable cell population in these tau transgenic mice, have elongated morphology (Fig. 1B, tau, arrowheads). Quantitative analysis reveals a significant increase in mean mitochondrial length in hippocampal neurons from tau transgenic mice (Fig. 1B, graph). We observe similar mitochondrial elongation in a second murine model of tauopathy, K3, in which the FTDP-17 associated mutant form of tau carrying the K369I mutation is expressed under the control of the mThy1.2 promoter (Ittner et al., 2008). Mitochondrial elongation is prominent in frontal cortical neurons, which express high levels of tau in these animals (Fig. S1F). 3D reconstruction of confocal fluorescence Z-stacks captured from *Drosophila* and murine neurons affords a more detailed view of the elongated morphology and interconnected organization of mitochondria induced by human tau (Supplementary movies 1–4).

Reversing mitochondrial elongation rescues neurotoxicity in vivo

To determine if toxicity of tau to postmitotic neurons is influenced by the mitochondrial elongation we observe in animal models, we manipulated the mitochondrial dynamics machinery genetically. We focused on DRP1 and MARF (the fly homolog of mammalian MFN), and increased and decreased expression of each protein. To increase net mitochondrial fission levels we overexpressed DRP1 and decreased levels of MARF using transgenic RNAi. These modifications significantly reduce mitochondrial length in tau transgenic flies (Fig. 2A). Importantly, normalization of mitochondrial length is accompanied by significant rescue of neurotoxicity, as monitored with TUNEL staining to identify dying neurons (Fig. 2B). Reduction of MARF or increase of DRP1 does not produce significant mitochondrial shortening or neuronal toxicity in the absence of human tau expression using the genetic modifiers indicated.

We then performed genetic manipulations that altered dynamics in the reciprocal fashion, toward increased fusion, by overexpressing MARF or reducing DRP1 through transgenic RNAi. When we increase fusion, we observe a further increase in mitochondrial length in tau transgenic flies. Enhanced mitochondrial elongation is accompanied by significantly increased neurodegeneration (Fig. 2B). To validate the effects of DRP1 and MARF depletion by RNAi, we used a loss of function *DRP1* mutant ($DRP1^{T26}$; Verstreken et al., 2005) and a chromosomal deficiency for the *MARF* locus (*MARF def.*; Parks et al., 2004), both of which modify mitochondrial length and neurotoxicity in tau transgenic flies (Fig. S2B,C). We also find that a loss-of-function mutation in *OPA1-like* ($OPA1\text{-}like^{S3475}$, Spradling et al., 1999), the fly homolog of the mammalian *OPA1* fusion gene, normalizes mitochondrial length and suppresses toxicity in our *Drosophila* tauopathy model (Fig. S2B,C). No significant effect on mitochondrial morphology or neurodegeneration is observed when DRP1 is reduced in the absence of transgenic human tau expression, consistent with the relatively modest reduction of *DRP1* expression induced by transgenic RNAi (Fig. S2D). More severe reductions of DRP1 levels cause lethality (Verstreken et al., 2005). In contrast, overexpression of MARF in the absence of tau produces elongation of mitochondria (Fig. 2A), and also increases TUNEL staining modestly, but significantly, above baseline (Fig. 2B), supporting the sensitivity of postmitotic neurons to disruption of normal mitochondrial dynamics. These genetic data, taken together, provide strong support for a causal relationship between the mitochondrial elongation observed in tau transgenic flies and tau neurotoxicity.

Oxidative stress promotes neurotoxicity in the *Drosophila* model of tauopathy used here (Dias-Santagata et al., 2007) and increased ROS production has been associated with mitochondrial dysfunction in tau transgenic mice (David et al., 2005). To determine if abnormal mitochondrial morphology correlates with oxidative stress we monitored ROS

production in whole mount brains using the superoxide-dependent fluorescent probe dihydroethidium (DHE, Chang and Min, 2005). Brains from animals expressing tau show a significant increase in superoxide production compared with brains from controls (Fig. 2C). Abnormal superoxide production is reduced toward baseline by increasing DRP1 and reducing MARF, manipulations that normalize mitochondrial length and prevent neuronal death. Conversely, superoxide production is further increased in tau transgenic flies by MARF overexpression and RNAi-mediated knockdown of DRP1 (Fig. 2C).

In our model, oxidative stress is followed by abnormal activation of the cell cycle in postmitotic neurons, which promotes cell (Khurana et al., 2006; Dias-Santagata et al., 2007). To monitor cell cycle activation in the brains of tau transgenic flies we immunostained for proliferating cell nuclear antigen (PCNA), an S phase marker abnormally reexpressed in human AD tissue (Busser et al., 1998) as well as tau transgenic flies (Khurana et al., 2006). Overexpression of DRP1 or knockdown of MARF suppresses cell cycle activation (Fig. 2D). Conversely, MARF overexpression and DRP1 knockdown increase cell cycle activation in brains of tau transgenic flies. Western blot analysis shows no alteration in levels of tau in genetically modified backgrounds, confirming that manipulation of DRP1 and MARF do not alter toxicity of tau by simply increasing or decreasing the expression of the tau transgene (Fig. S2A).

Tau expression blocks mitochondrial localization of DRP1

We next explored the mechanism by which tau expression promotes mitochondrial elongation. We first evaluated expression of *DRP1* and *MARF* by real-time PCR, but did not observe changes in mRNA levels (Fig. S3A). We then examined the subcellular localization of DRP1. Cytoplasmic DRP1 protein must translocate to the mitochondria to drive fission (Frank et al., 2001). To visualize DRP1 in *Drosophila*, we used a transgenic strain carrying a 9.35 kb genomic rescue construct that has an in-frame FLAG-FIAsH-HA tag after the start codon of *DRP1* (Verstreken et al., 2005). The presence of this genomic rescue construct does not have a statistically significant effect on tau expression, mitochondrial length, or neuronal toxicity (Figs. S2A, S3B,C), consistent with modest expression of *DRP1* from its endogenous promoter (Fig. S2D). Visualizing DRP1 by immunostaining for HA we find that in control neurons DRP1 signal appears in discrete foci, almost exclusively localized to mitochondria (Fig. 3A, control, arrowheads). Immunostaining for FLAG shows an equivalent DRP1 staining pattern (Fig. S3D). However, in neurons from tau transgenic animals DRP1 foci are infrequent, and the majority of mitochondria do not colocalize with DRP1 (Fig. 3A, tau, arrowheads). Signal intensity profiles for DRP1 and mitoGFP verify the tau-mediated inhibition of colocalization (Fig. S3E). One possible explanation for the lack of DRP1 localization to mitochondria in tau transgenic neurons is that elongated mitochondria fail to recruit DRP1 normally. To test this idea we expressed MARF in the absence of tau. In neurons overexpressing MARF we observe the expected increase in mitochondrial length. However, in contrast to results from tau transgenic animals, elongated mitochondria in *MARF* transgenics do colocalize with DRP1 puncta (Fig. 3A, MARF, arrowheads). Thus, failure of DRP1 to localize to mitochondria in tau transgenic neurons is not likely to be a secondary effect of the mitochondrial elongation itself. Mitochondrial localization of DRP1 is also retained following MARF knockdown, as well as increased or decreased expression of DRP1 (Fig. S3F). To confirm that tau expression alters DRP1 localization, we isolated cytoplasmic and mitochondrial fractions from heads of flies expressing HA-tagged DRP1, and monitored DRP1 localization using an antibody directed to the HA epitope. DRP1 levels are equivalent in the total homogenate and cytoplasmic fraction of control and tau flies. However, the mitochondrial fraction shows specific depletion of DRP1 in tau transgenic flies (Fig. 3B). Similarly, fractionation of control and rTg4510 mouse hippocampus reveals reduced DRP1

in mitochondrial fractions from tau transgenic mice compared to controls (Fig. 3C). Immunoblotting for porin, a mitochondrial membrane protein, and GAPDH are used to confirm enrichment of mitochondrial and cytoplasmic proteins, respectively, during the fractionation procedure.

Actin stabilization blocks mitochondrial localization of DRP1

We have previously demonstrated that tau binds to and stabilizes actin. Excess actin stabilization by tau is required for neurotoxicity (Fulga et al., 2006). To determine if increasing F-actin level alters DRP1 localization we overexpressed the actin nucleating factor WASP using a *UAS-WASP* transgene (Berger et al., 2008). We also increased expression of the actin bundling protein forked. *forked* gene dosage was increased with a genomic rescue construct (Grieshaber et al., 2001). We first used the F-actin sensitive dye rhodamine-phalloidin in whole mount brains to confirm that WASP and forked increase F-actin (Fig. S4A). We then determined if stabilizing the actin cytoskeleton influences mitochondrial morphology and DRP1 localization to mitochondria. We find that compared to normal control mitochondria, mitochondria in neurons with increased expression of WASP or forked are frequently elongated (Fig. 4A, arrows). Elongated mitochondria often fail to colocalize with DRP1, while normal round to tubular mitochondria maintain DRP1 localization (Fig. 4A, arrowheads). Quantitative analysis demonstrates a significant increase in mitochondrial length resulting from overexpression of WASP or forked (Fig. 4A, graph). As would be expected, increasing the expression of WASP or forked together with human tau markedly enhances mitochondrial elongation and neuronal toxicity, without altering tau expression (Fig. S4B,C, Fig. S2A). Subcellular fractionation confirms reduced localization of DRP1 to mitochondria with increased *forked* gene dosage (Fig. 4B).

To investigate a possible physical interaction between DRP1 and F-actin, we isolated F-actin from head homogenates of control and forked-overexpressing flies by precipitation with biotinylated phalloidin. Western blotting shows that DRP1 coprecipitates with F-actin. Stabilization of actin by forked overexpression substantially increases the amount of DRP1 coprecipitated with biotinylated phalloidin (Fig. 4C). These findings support a direct or close physical interaction between F-actin and DRP1, and are consistent with accumulation of DRP1 on F-actin and concomitant depletion of mitochondrial DRP1 in response to increased actin stabilization.

Reversing actin stabilization rescues tau-induced mitochondrial defects

Since tau stabilizes actin (Fulga et al., 2006), and actin stabilization inhibits mitochondrial localization of DRP1, we postulated that tau exerts its effects on mitochondrial structure and function via excessive actin stabilization. To test our hypothesis directly we destabilized actin in the presence of tau and monitored the effects on mitochondrial morphology, DRP1 localization, and neurotoxicity. To destabilize actin we expressed the actin severing protein gelsolin (Yin and Stossel, 1979) using a *UAS-gelsolin* transgene. We first confirmed that expression of gelsolin reduces F-actin levels by staining whole mount brain preparations with rhodamine-phalloidin (Fig. S5). Overexpression of gelsolin reduces mean mitochondrial length, rescues neurodegeneration, and decreases ROS production in tau transgenic neurons (Fig. 5A). We also find increased localization of DRP1 to mitochondria when gelsolin is coexpressed with tau (Fig. 5B, arrowheads) and reduced incidence of elongated mitochondria lacking DRP1 association (Fig. 5B, arrows). These findings overall provide strong evidence that tau blocks DRP1 localization to mitochondria through its influence on the actin cytoskeleton.

Actin and myosin are required for localization of DRP1 to mitochondria

We wondered if actin stabilization might play a more general role in controlling the subcellular localization of DRP1. We thus examined the localization of DRP1 and F-actin in Cos-1 cells, an immortalized mammalian fibroblastic cell line. Visualization of F-actin using rhodamine-phalloidin and endogenous DRP1 by immunofluorescence with a DRP1 antibody reveals colocalization of DRP1 with actin stress fibers (Fig. S6A). We next examined the effects of actin stabilization on DRP1 and mitochondria in these cells, using transient transfection of the actin stabilizing protein transgelin (Shapland et al., 1993). We first confirmed that expression of transgelin increases levels of F-actin by staining with rhodamine-phalloidin (Fig. S6B). Visualizing DRP1 by immunofluorescence and mitochondria by transfection of mitochondrially-directed red fluorescent protein (mitoRFP), we find that in control cells mitochondria are round or modestly tubular, and DRP1 colocalizes with mitochondria (Fig. 6A, control, inset). In contrast, in transgelin-expressing cells mitochondria are elongated, and DRP1 shows less mitochondrial colocalization (Fig. 6A, transgelin, inset). Quantitative analysis reveals a significant increase in mean mitochondrial length in transgelin-expressing cells compared with controls (Fig. 6A, graph). 3D reconstruction of confocal fluorescence Z stacks verifies mitochondrial elongation in response to transgelin transfection (Supplementary movies 5 and 6). Signal intensity profiles confirm loss of association between mitochondria and DRP1 following transgelin expression (Fig. S6C).

We next assessed whether these changes in mitochondria morphology correlate with a disruption of mitochondrial bioenergetics. Measuring mitochondrial membrane potential using the TMRM dye, we find that transgelin transfection induces a significant reduction in membrane potential compared with control (Fig. 6B). Mitochondrial elongation, mislocalization of DRP1, and reduced mitochondrial membrane potential also occur in response to transient transfection of tau (Fig. S6D,E), comparable to the effects of expressing tau in *Drosophila* neurons. These findings confirm our observation of F-actin-mediated disruption of DRP1 localization in *Drosophila* and suggest that F-actin has a fundamental regulatory role in DRP1 localization and maintenance of proper mitochondrial function.

We next turned our focus to potential mediators of actin-dependent localization of DRP1 to mitochondria. Several members of the myosin family of actin-based motor proteins can link proteins and organelles with actin cables (Akhmanova and Hammer, 2010). Screening loss-of-function mutations in eight neuronally-expressed *Drosophila* myosins, we identified myosin II as a regulator of mitochondrial fission in fly neurons. Zipper (zip) and spaghetti squash (sqh) are the *Drosophila* homologs of the mammalian myosin II heavy chain and regulatory light chain, respectively. We found that flies heterozygous for a loss of function allele of either *zip* (*zip*^{1}, Zhao et al., 1988) or *sqh* (*sqh*^{AX3}, Jordan and Karess, 1997) have increased numbers of elongated neuronal mitochondria (Fig. 7A, arrows). Elongated mitochondria in *zip*^{1} or *sqh* ^{AX3} mutants rarely colocalize with DRP1, while normal round to tubular mitochondria maintain DRP1 colocalization (Fig. 7A, arrowheads). Quantitative analysis confirms a significant increase in mitochondrial length with reduced levels of zip or sqh (Fig. 7A, graph). Mutation of either *sqh* or *zip* enhances tau-mediated mitochondrial elongation and neurotoxicity, without altering tau expression (Fig. S7A,B, Fig. S2A). Subcellular fractionation confirms reduced localization of DRP1 to mitochondria in *zip*^{1} and *sqh*^{AX3} flies compared to controls, despite comparable levels of DRP1 in the cytoplasm (Fig. 7B,C). These findings demonstrate a requirement for myosin II in localizing DRP1 to mitochondria.

To further characterize the contribution of myosin II to mitochondrial fission, we examined the interaction of myosin II, F-actin, and mitochondria. A small volume of total actin is

consistently observed in the mitochondrial fraction following a stringent fractionation procedure from fly head homogenate, suggesting the retention of mitochondria-bound actin. Mitochondria-bound actin is reduced in both *zip*^{1} and *sqh*^{AX3} mutant flies (Fig. 8A,B, Mitochondria, input). Using biotinylated phalloidin to precipitate F-actin from mitochondrial fractions, we find that the level of mitochondria-associated F-actin is also reduced by both *zip*^{1} and *sqh*^{AX3} (Fig. 8A,B, Mitochondria, BiotPh Precip). In cytoplasmic fractions, the levels of total actin and precipitated F-actin are equivalent between control and either *zip*^{1} or *sqh*^{AX3} mutants (Fig. 8A,B, Cytoplasm). In *zip*^{1} and *sqh*^{AX3} flies, reduced association of mitochondria with F-actin correlates with increased association of DRP1 with F-actin, observed by coprecipitation of F-actin and DRP1 from total head homogenate using biotinylated-phalloidin (Fig. 8C,D). These findings suggest that myosin II facilitates tethering of mitochondria to F-actin, a connection that is required for mitochondria to interact with DRP1.

To determine if myosin II has a general and conserved role in DRP1 localization, we focused on the regulatory light chain, MLC2. We transfected Cos-1 cells with siRNA targeting two independent, non-overlapping sequences in *MLC2*. We first confirmed depletion of MLC2 protein by western blot analysis (Fig. S8B). We then assessed mitochondrial morphology and the subcellular localization of DRP1. In control cells, mitochondria, detected with transfected mitoRFP, are round or slightly tubular and colocalize with DRP1. In *MLC2* siRNA-transfected cells, mitochondria are significantly elongated, and DRP1 signal is diffuse (Fig. 8E, insets, graph). MLC2 is phosphorylated by myosin light chain kinase (MLCK), which is essential to MLC2 activity (Watanabe et al., 2007). Treatment of cells with ML-7, a chemical inhibitor of MLCK, recapitulates the effects of *MLC2* RNAi on mitochondrial morphology and DRP1 localization (Fig. S8A, insets, graph). These results support a conserved interaction among DRP1, myosin, and actin.

Discussion

Here we describe a previously unsuspected target for tau neurotoxicity in human neurodegenerative disease: mislocalization of the mitochondrial fission protein DRP1 with subsequent failure of normal mitochondrial dynamics control. Our current data extends a model of the cascade of neurotoxicity triggered by accumulation of human tau. Previous work from our laboratories and others (Ahlijanian et al., 2000; Noble et al., 2005; Steinhilb et al., 2007a; Steinhilb et al., 2007b; Iijima-Ando et al., 2010) places phosphorylation of tau upstream in a sequence of cellular events, including actin stabilization (Fulga et al., 2006), that leads to neuronal death. Our new results place tau phosphorylation upstream of altered mitochondrial dynamics (Fig. S1), and further indicate that proper regulation of the actin cytoskeleton is critical for localization of DRP1 to mitochondria and subsequent mitochondrial fission.

Here we show a physical interaction between F-actin and DRP1. Further, we find that myosin II is required for both localization of mitochondria to actin, and DRP1 to mitochondria (Figs. 7,8). These results support a model in which DRP1 and mitochondria are recruited to F-actin, followed by actin-based translocation leading to mitochondrial localization of DRP1 and subsequent mitochondrial fission. Excess actin stabilization inhibits translocation and colocalization of DRP1 and mitochondria, resulting in mitochondrial elongation (Fig. S8C). Having observed F-actin dependent mislocalization of DRP1 following tau expression (Figs. 3 and 5), we propose that tau-mediated actin stabilization (Fulga et al., 2006) is sufficient to mislocalize DRP1.

Previous studies have demonstrated reduced organelle motility following excessive F-actin stabilization (Chada and Hollenbeck, 2004; Semenova et al., 2008). Also supporting our model, myosin II-mediated linkage of mitochondria with actin has recently been reported (Reyes et al., 2011), and mitochondria have been shown to undergo myosin-mediated transport on actin filaments in mammalian cells (Quintero et al., 2009). Alternatively, excessive F-actin within the cell might sequester DRP1 away from mitochondria. However, we do not favor this second model because destabilization of actin, like excessive stabilization, causes DRP1 mislocalization and mitochondrial elongation, as documented here (Fig. 5) and previously reported by De Vos et al. (2005).

Importantly, the mechanisms we outline here appear to be general ones. We observe altered mitochondrial dynamics following expression of not only FTDP-17 associated forms of tau (Fig. 1), but with expression of wild type human tau as well (Fig. S1). Neurodegenerative tauopathies are characterised by deposition of both wild type and mutant forms of tau. Although our studies were motivated by findings in our *Drosophila* model of tauopathy, our consistent results from two mouse models of tauopathy (Figs. 1, S1, and 3) argue for a conserved mechanism of tau neurotoxicity in vertebrate systems. Similarly, while tau is expressed primarily in neurons, the actin- and myosin-dependence of DRP1 localization to mitochondria and subsequent mitochondrial fission is most likely a general mechanism regulating mitochondrial dynamics, as demonstrated by our experiments in Cos-1 cells (Figs. 6 and 8).

There may be additional mechanisms perturbing mitochondrial dynamics in AD and related tauopathies. Fibroblasts from patients with AD have been shown to have abnormally long mitochondria. However, in contrast to our findings, DRP1 expression is reduced in these fibroblasts (Wang et al., 2008). Increased levels of S-nitrosylated DRP1 have been observed in brains from patients with AD, although biochemical analysis supports an activating, rather than inactivating, influence of oxidatively modified DRP1 (Cho et al., 2009). The phosphorylation state of DRP1 contributes to mitochondrial localization, and is regulated by a number of kinases and phosphatases including PKA and calcineurin (Merrill et al., 2011; Cereghetti et al., 2008). Interestingly, inhibition of both PKA and calcineurin has been observed in AD (Shi et al., 2011; Cook et al., 2005).

Our current findings are consistent with an important role for properly regulated DRP1 function in maintaining postmitotic neuronal populations, and raise the important question of the cellular mechanisms mediating neurodegeneration in response to inadequate fission. A growing literature suggests that fission is an important mechanism promoting segregation and eventual removal of mitochondria with reduced membrane potential by autophagy (Twig et al., 2008). Of note, mutations in the parkinsonian syndrome-related proteins parkin and PINK1 reveal an apparent function in the mitochondrial quality control pathway (Youle and Narendra, 2011). Impaired mitochondrial fission has also been associated with altered mitochondrial bioenergetics (Parone et al., 2008). Indeed, we find excess production of ROS in tau flies with elongated mitochondria. We have previously shown that oxidative stress plays a critical role in the neurotoxicity of tau (Dias-Santagata et al., 2007). We have further shown that DNA damage leads to inappropriate cell cycle activation and subsequent neuronal apoptosis (Khurana et al., 2006; Khurana et al., 2011). Thus, excess production of ROS following insufficient mitochondrial fission represents a plausible downstream mechanism mediating neurodegeneration caused by somatodendritic tau accumulation.

In addition to a general disruption of oxidative metabolism within the cell, there may be neuronal-specific mechanisms that promote neuronal toxicity downstream of inadequate fission. Mitochondria have important functions locally at synapses, including calcium buffering and ATP production, linking neuronal survival to transport of mitochondria from

the point of biogenesis in the soma to distal synaptic sites (Otera and Mihara, 2011). A number of studies have suggested that increased expression or altered microtubule binding of tau may compromise axonal transport of a range of cargo, including mitochondria (Ebneth et al., 1998; Dixit et al., 2008; Ittner et al., 2009; Kopeikina et al., 2011). Consistent with these findings, we show here that transgenic RNAi-mediated knockdown of *miro*, which facilitates linkage of mitochondria to kinesin for axonal transport (Glater et al., 2006), enhances tau toxicity (Fig. S2). However, our data further suggests that the alteration in mitochondrial dynamics we observe is not a secondary consequence of impaired axonal transport (Fig. 1). In the context of AD, the most common tauopathy, toxicity of Abeta peptides may further compromise mitochondrial function (Eckert et al., 2008). Thus, in patients, multiple pathways acting in series and in parallel may disrupt mitochondrial homeostasis. Our current findings strongly suggest F-actin mediated disruption of mitochondrial fission as an important step in the cellular cascade that promotes neuronal dysfunction and death in neurodegenerative diseases associated with tau pathology.

Experimental Procedures

Genetics

All fly crosses and aging were performed at 25°C. TUNEL, PCNA, mitochondrial length quantification, and ROS production were assessed in 10-day-old flies, except where noted (Figure S1). Tau transgenic mice of the strain rTg4510 (Ramsden et al., 2005; Santacruz et al., 2005) were analyzed at 7 months of age and K3 (Ittner et al., 2008) at 10 months of age. Controls were littermates not carrying the rTg4510 or K3 transgenes. *Drosophila* cDNAs for *DRP1* (AT04516), *MARF* (RE04414), and *gelsolin* (SD07495) were from the *Drosophila* Genomics Resource Center, and were cloned into the pUAST vector. Transgenic strains were created by embryo injection. The panneural driver e*lav-GAL4* was used in all fly experiments. We have described the human *UAS-tau*^{R406W}, *UAS-tau*^{WT}, *UAS-tau*^{E14} transgenic lines previously (Wittmann et al., 2001; Khurana et al., 2006). Clones homozygous for the null mutation *milton*^{92} were generated using the MARCM system (Lee and Luo, 1999). The following stocks were obtained from the Bloomington *Drosophila* stock center: e*lav-GAL4*, *UAS-MARF RNAi* (TRiP.JF01650), *Df(1)Exel6239 (MARF def.)*, *DRP1*^{T26}, *OPA1-like*^{S3475}, *forked*$^{+t13}$, *zip*^{1}, *sqh*^{AX3}. Transgenic lines expressing siRNA directed to DRP1 (line #44155) and *miro* (line #106683) were from the Vienna *Drosophila* RNAi Center. Transgenic lines were created in the *w*^{1118} background. The following lines were kindly provided by the indicated investigators: *UAS-WASP,* Eyal Schejter; *UAS-mitoGFP*, *milton*^{92}, Thomas Schwarz; *FLAG-FlAsH-HA-DRP1,* Hugo Bellen.

Cell culture and transfection

Transient transfection of plasmid DNA and siRNA was performed using Lipofectamine 2000 (Invitrogen) according to manufacturer's instructions. TMRM and CCCP were purchased from Invitrogen, ML-7 from Sigma. MitoRFP and transgelin cDNAs were provided by Tom Schwarz and William Dynan, respectively, and were expressed using the pCDNA expression vector. *MLC2* and negative control siRNA (ID# s9180, s224081, AM4611) were purchased from Applied Biosystems.

Immunocytochemistry and histology

Paraffin sections from adult *Drosophila* heads and mouse brains were used for immunostaining experiments, and secondary detection was performed using fluorescently labeled secondary antibodies. Neuronal apoptosis was assayed by nuclear DNA fragmentation indicated by TUNEL staining using a commercially available kit (TdT FragEL, Calbiochem). TUNEL-positive cells were counted throughout the entire brain.

Confocal Microscopy

To assess mitochondrial length, *Drosophila* Kenyon neurons, murine hippocampal pyramidal neurons, and Cos-1 cells were imaged by laser-scanning confocal microscopy. In two-dimensional projections of confocal *z*-stacks, individual mitochondrion length was measured by freehand line length in ImageJ (http://rsbweb.nih.gov/ij). F-actin levels were determined in adult fly brains as previously described (Fulga et al., 2006). Superoxide levels were measured in adult fly brains using dihydroethidium (Invitrogen).

Mitochondrial fractionation

Fly heads or isolated mouse hippocampi were homogenized and centrifuged at 800xg to pellet debris, and the supernatant collected and centrifuged at 11,000xg to yield a pellet containing mitochondria and supernatant containing cytoplasmic proteins. One-day-old flies were used.

Phalloidin precipitation

Fly heads were homogenized and centrifuged at 800xg to pellet debris. The supernatant was incubated with 0.3 units biotinylated-phalloidin (Molecular Probes) followed by precipitation with streptavidin-coupled Dynabeads (Invitrogen). To control for nonspecific protein interactions, the same protocol was followed with biotin in place of biotinylated phalloidin. Flies were 1 day old in all coprecipitations.

Immunoblotting

Samples were analyzed by 15% SDS-PAGE and immunoblotted according to standard protocols. All immunoblots were repeated at least three times with similar results. See Supplementary Information for detailed methods.

Supplementary Material

Refer to Web version on PubMed Central for supplementary material.

Acknowledgments

We thank D. Kiehart for the squash antibody and W. Dynan and T. Schwarz for providing cDNAs. The rTg4510 mice were a generous gift of Bradley Hyman. T. Schwarz, E. Schejter, and H. Bellen kindly provided *Drosophila* stocks. D. Rennie at the Cutaneous Biology Research Center at Massachusetts General Hospital performed embryo injections to create transgenic strains. Confocal microscopy was performed at the Harvard Neurodiscovery Center Optical Imaging Facility. We thank T. Fulga and M. Colaiácovo for helpful discussions. The work was supported by grants from the NIA and Ellison Medical Foundation to M.B.F., NIA to B.D., and the Clem Jones Foundation to J.G.

References

Ahlijanian MK, Barrezueta NX, Williams RD, Jakowski A, Kowsz KP, McCarthy S, Coskran T, Carlo A, Seymour PA, Burkhardt JE, Nelson RB, McNeish JD. Hyperphosphorylated tau and neurofilament and cytoskeletal disruptions in mice overexpressing human p25, an activator of cdk5. Proc Natl Acad Sci U S A. 2000; 97:2910–2915. [PubMed: 10706614]

Akhmanova A, Hammer JA 3rd. Linking molecular motors to membrane cargo. Curr Opin Cell Biol. 2010; 22:479–487. [PubMed: 20466533]

Alexander C, Votruba M, Pesch UE, Thiselton DL, Mayer S, Moore A, Rodriguez M, Kellner U, Leo-Kottler B, Auburger G, Bhattacharya SS, Wissinger B. OPA1, encoding a dynamin-related GTPase, is mutated in autosomal dominant optic atrophy linked to chromosome 3q28. Nat Genet. 2000; 26:211–215. [PubMed: 11017080]

Berger S, Schafer G, Kesper DA, Holz A, Eriksson T, Palmer RH, Beck L, Klambt C, Renkawitz-Pohl R, Onel SF. WASP and SCAR have distinct roles in activating the Arp2/3 complex during myoblast fusion. J Cell Sci. 2008; 121:1303–1313. [PubMed: 18388318]

Brand AH, Perrimon N. Targeted gene expression as a means of altering cell fates and generating dominant phenotypes. Development. 1993; 118:401–15. [PubMed: 8223268]

Bratic I, Trifunovic A. Mitochondrial energy metabolism and ageing. Biochim Biophys Acta. 2010; 1797:961–967. [PubMed: 20064485]

Busser J, Geldmacher DS, Herrup K. Ectopic cell cycle proteins predict the sites of neuronal cell death in Alzheimer's disease brain. J Neurosci. 1998; 18:2801–2807. [PubMed: 9525997]

Cereghetti GM, Stangherlin A, Martins de Brito O, Chang CR, Blackstone C, Bernardi P, Scorrano L. Dephosphorylation by calcineurin regulates translocation of Drp1 to mitochondria. Proc Natl Acad Sci U S A. 2008; 105:15803–15808. [PubMed: 18838687]

Chada SR, Hollenbeck PJ. Nerve growth factor signaling regulates motility and docking of axonal mitochondria. Curr Biol. 2004; 14:1272–1276. [PubMed: 15268858]

Chang KT, Min KT. Drosophila melanogaster homolog of Down syndrome critical region 1 is critical for mitochondrial function. Nat Neurosci. 2005; 8:1577–1585. [PubMed: 16222229]

Chen H, Detmer SA, Ewald AJ, Griffin EE, Fraser SE, Chan DC. Mitofusins Mfn1 and Mfn2 coordinately regulate mitochondrial fusion and are essential for embryonic development. J Cell Biol. 2003; 160:189–200. [PubMed: 12527753]

Cho DH, Nakamura T, Fang J, Cieplak P, Godzik A, Gu Z, Lipton SA. S-nitrosylation of Drp1 mediates beta-amyloid-related mitochondrial fission and neuronal injury. Science. 2009; 324:102–105. [PubMed: 19342591]

Cipolat S, Martins de Brito O, Dal Zilio B, Scorrano L. OPA1 requires mitofusin 1 to promote mitochondrial fusion. Proc Natl Acad Sci U S A. 2004; 101:15927–15932. [PubMed: 15509649]

Cook CN, Hejna MJ, Magnuson DJ, Lee JM. Expression of calcipressin1, an inhibitor of the phosphatase calcineurin, is altered with aging and Alzheimer's disease. J Alzheimers Dis. 2005; 8:63–73. [PubMed: 16155351]

David DC, Hauptmann S, Scherping I, Schuessel K, Keil U, Rizzu P, Ravid R, Drose S, Brandt U, Muller WE, Eckert A, Gotz J. Proteomic and functional analyses reveal a mitochondrial dysfunction in P301L tau transgenic mice. J Biol Chem. 2005; 280:23802–23814. [PubMed: 15831501]

De Vos KJ, Allan VJ, Grierson AJ, Sheetz MP. Mitochondrial function and actin regulate dynamin-related protein 1-dependent mitochondrial fission. Curr Biol. 2005; 15:678–683. [PubMed: 15823542]

Delettre C, Lenaers G, Griffoin JM, Gigarel N, Lorenzo C, Belenguer P, Pelloquin L, Grosgeorge J, Turc-Carel C, Perret E, et al. Nuclear gene OPA1, encoding a mitochondrial dynamin-related protein, is mutated in dominant optic atrophy. Nat Genet. 2000; 26:207–210. [PubMed: 11017079]

Dias-Santagata D, Fulga TA, Duttaroy A, Feany MB. Oxidative stress mediates tau-induced neurodegeneration in Drosophila. J Clin Invest. 2007; 117:236–245. [PubMed: 17173140]

Dixit R, Ross JL, Goldman YE, Holzbaur EL. Differential regulation of dynein and kinesin motor proteins by tau. Science. 2008; 319:1086–1089. [PubMed: 18202255]

Ebneth A, Godemann R, Stamer K, Illenberger S, Trinczek B, Mandelkow E. Overexpression of tau protein inhibits kinesin-dependent trafficking of vesicles, mitochondria, and endoplasmic reticulum: implications for Alzheimer's disease. J Cell Biol. 1998; 143:777–794. [PubMed: 9813097]

Eckert A, Hauptmann S, Scherping I, Meinhardt J, Rhein V, Drose S, Brandt U, Fandrich M, Muller WE, Gotz J. Oligomeric and fibrillar species of beta-amyloid (A beta 42) both impair mitochondrial function in P301L tau transgenic mice. J Mol Med (Berl). 2008; 86:1255–1267. [PubMed: 18709343]

Frank S, Gaume B, Bergmann-Leitner ES, Leitner WW, Robert EG, Catez F, Smith CL, Youle RJ. The role of dynamin-related protein 1, a mediator of mitochondrial fission, in apoptosis. Dev Cell. 2001; 1:515–525. [PubMed: 11703942]

Fulga TA, Elson-Schwab I, Khurana V, Steinhilb ML, Spires TL, Hyman BT, Feany MB. Abnormal bundling and accumulation of F-actin mediates tau-induced neuronal degeneration in vivo. Nat Cell Biol. 2006; 9:139–148. [PubMed: 17187063]

Glater EE, Megeath LJ, Stowers RS, Schwarz TL. Axonal transport of mitochondria requires milton to recruit kinesin heavy chain and is light chain independent. J Cell Biol. 2006; 173:545–557. [PubMed: 16717129]

Grieshaber SS, Lankenau DH, Talbot T, Holland S, Petersen NS. Expression of the 53 kD forked protein rescues F-actin bundle formation and mutant bristle phenotypes in Drosophila. Cell Motil Cytoskeleton. 2001; 50:198–206. [PubMed: 11807940]

Hardy J, Selkoe DJ. The amyloid hypothesis of Alzheimer's disease: progress and problems on the road to therapeutics. Science. 2002; 297:353–356. [PubMed: 12130773]

Hirai K, Aliev G, Nunomura A, Fujioka H, Russell RL, Atwood CS, Johnson AB, Kress Y, Vinters HV, Tabaton M, et al. Mitochondrial Abnormalities in Alzheimer's Disease. J Neurosci. 2001; 21:3017–3023. [PubMed: 11312286]

Hutton M, Lendon CL, Rizzu P, Baker M, Froelich S, Houlden H, Pickering-Brown S, Chakraverty S, Isaacs A, Grover A, et al. Association of missense and 5[prime]-splice-site mutations in tau with the inherited dementia FTDP-17. Nature. 1998; 393:702–705. [PubMed: 9641683]

Hwa JJ, Hiller MA, Fuller MT, Santel A. Differential expression of the Drosophila mitofusin genes fuzzy onions (fzo) and dmfn. Mech Dev. 2002; 116:213–216. [PubMed: 12128227]

Iijima-Ando K, Zhao L, Gatt A, Shenton C, Iijima K. A DNA damage-activated checkpoint kinase phosphorylates tau and enhances tau-induced neurodegeneration. Hum Mol Genet. 2010; 19:1930–1938. [PubMed: 20159774]

Ittner LM, Fath T, Ke YD, Bi M, van Eersel J, Li KM, Gunning P, Gotz J. Parkinsonism and impaired axonal transport in a mouse model of frontotemporal dementia. Proc Natl Acad Sci U S A. 2008; 105:15997–16002. [PubMed: 18832465]

Ittner LM, Ke YD, Gotz J. Phosphorylated Tau interacts with c-Jun N-terminal kinase-interacting protein 1 (JIP1) in Alzheimer disease. J Biol Chem. 2009; 284:20909–20916. [PubMed: 19491104]

Ittner LM, Gotz J. Amyloid-beta and tau - a toxic pas de deux in Alzheimer's disease. Nat Rev Neurosci. 2010

Jackson GR, Wiedau-Pazos M, Sang TK, Wagle N, Brown CA, Massachi S, Geschwind DH. Human wild-type tau interacts with wingless pathway components and produces neurofibrillary pathology in Drosophila. Neuron. 2002; 34:509–519. [PubMed: 12062036]

Jordan P, Karess R. Myosin light chain-activating phosphorylation sites are required for oogenesis in Drosophila. J Cell Biol. 1997; 139:1805–1819. [PubMed: 9412474]

Khurana V, Lu Y, Steinhilb ML, Oldham S, Shulman JM, Feany MB. TOR-Mediated Cell-Cycle Activation Causes Neurodegeneration in a Drosophila Tauopathy Model. Current Biology. 2006; 16:230–241. [PubMed: 16461276]

Khurana V, Elson-Schwab I, Fulga TA, Sharp KA, Loewen CA, Mulkearns E, Tyynela J, Scherzer CR, Feany MB. Lysosomal dysfunction promotes cleavage and neurotoxicity of tau in vivo. PLoS Genet. 2010; 6:e1001026. [PubMed: 20664788]

Khurana V, Merlo P, DuBoff B, Fulga TA, Sharp KA, Campbell SD, Gotz J, Feany MB. A neuroprotective role for the DNA damage checkpoint in tauopathy. Aging Cell. 2011 in press.

Kopeikina KJ, Carlson GA, Pitstick R, Ludvigson AE, Peters A, Luebke JI, Koffie RM, Frosch MP, Hyman BT, Spires-Jones TL. Tau accumulation causes mitochondrial distribution deficits in neurons in a mouse model of tauopathy and in human Alzheimer's disease brain. Am J Pathol. 2011; 179:2071–2082. [PubMed: 21854751]

Lee T, Luo L. Mosaic analysis with a repressible cell marker for studies of gene function in neuronal morphogenesis. Neuron. 1999; 22:451–461. [PubMed: 10197526]

Loewen CA, Feany MB. The unfolded protein response protects from tau neurotoxicity in vivo. PLoS One. 2010; 5:e13084. [PubMed: 20927324]

Merrill RA, Dagda RK, Dickey AS, Cribbs JT, Green SH, Usachev YM, Strack S. Mechanism of neuroprotective mitochondrial remodeling by PKA/AKAP1. PLoS Biol. 2011; 9:e1000612. [PubMed: 21526220]

Nishimura I, Yang Y, Lu B. PAR-1 kinase plays an initiator role in a temporally ordered phosphorylation process that confers tau toxicity in Drosophila. Cell. 2004; 116:671–682. [PubMed: 15006350]

Noble W, Planel E, Zehr C, Olm V, Meyerson J, Suleman F, Gaynor K, Wang L, LaFrancois J, Feinstein B, et al. Inhibition of glycogen synthase kinase-3 by lithium correlates with reduced tauopathy and degeneration in vivo. Proc Natl Acad Sci U S A. 2005; 102:6990–6995. [PubMed: 15867159]

Otera H, Mihara K. Molecular Mechanisms and Physiologic Functions of Mitochondrial Dynamics. J Biochem. 2011

Parks AL, Cook KR, Belvin M, Dompe NA, Fawcett R, Huppert K, Tan LR, Winter CG, Bogart KP, Deal JE, et al. Systematic generation of high-resolution deletion coverage of the Drosophila melanogaster genome. Nat Genet. 2004; 36:288–292. [PubMed: 14981519]

Parone PA, Da Cruz S, Tondera D, Mattenberger Y, James DI, Maechler P, Barja F, Martinou JC. Preventing mitochondrial fission impairs mitochondrial function and leads to loss of mitochondrial DNA. PLoS One. 2008; 3:e3257. [PubMed: 18806874]

Perry EK, Perry RH, Tomlinson BE, Blessed G, Gibson PH. Coenzyme A-acetylating enzymes in Alzheimer's disease: possible cholinergic 'compartment' of pyruvate dehydrogenase. Neurosci Lett. 1980; 18:105–110. [PubMed: 6133246]

Plassman BL, Langa KM, Fisher GG, Heeringa SG, Weir DR, Ofstedal MB, Burke JR, Hurd MD, Potter GG, Rodgers WL, et al. Prevalence of dementia in the United States: the aging, demographics, and memory study. Neuroepidemiology. 2007; 29:125–132. [PubMed: 17975326]

Poorkaj P, Bird TD, Wijsman E, Nemens E, Garruto RM, Anderson L, Andreadis A, Wiederholt WC, Raskind M, Schellenberg GD. Tau is a candidate gene for chromosome 17 frontotemporal dementia. Ann Neurol. 1998; 43:815–825. [PubMed: 9629852]

Quintero OA, DiVito MM, Adikes RC, Kortan MB, Case LB, Lier AJ, Panaretos NS, Slater SQ, Rengarajan M, Feliu M, Cheney RE. Human Myo19 is a novel myosin that associates with mitochondria. Curr Biol. 2009; 19:2008–2013. [PubMed: 19932026]

Ramsden M, Kotilinek L, Forster C, Paulson J, McGowan E, SantaCruz K, Guimaraes A, Yue M, Lewis J, Carlson G, Hutton M, Ashe KH. Age-dependent neurofibrillary tangle formation, neuron loss, and memory impairment in a mouse model of human tauopathy (P301L). J Neurosci. 2005; 25:10637–10647. [PubMed: 16291936]

Reyes A, He J, Mao CC, Bailey LJ, Di Re M, Sembongi H, Kazak L, Dzionek K, Holmes JB, Cluett TJ, et al. Actin and myosin contribute to mammalian mitochondrial DNA maintenance. Nucleic Acids Res. 2011; 39:5098–5108. [PubMed: 21398640]

Rhein V, Song X, Wiesner A, Ittner LM, Baysang G, Meier F, Ozmen L, Bluethmann H, Drose S, Brandt U, et al. Amyloid-beta and tau synergistically impair the oxidative phosphorylation system in triple transgenic Alzheimer's disease mice. Proc Natl Acad Sci U S A. 2009; 106:20057–20062. [PubMed: 19897719]

Santacruz K, Lewis J, Spires T, Paulson J, Kotilinek L, Ingelsson M, Guimaraes A, DeTure M, Ramsden M, McGowan E, et al. Tau suppression in a neurodegenerative mouse model improves memory function. Science. 2005; 309:476–481. [PubMed: 16020737]

Semenova I, Burakov A, Berardone N, Zaliapin I, Slepchenko B, Svitkina T, Kashina A, Rodionov V. Actin dynamics is essential for myosin-based transport of membrane organelles. Curr Biol. 2008; 18:1581–1586. [PubMed: 18951026]

Shapland C, Hsuan JJ, Totty NF, Lawson D. Purification and properties of transgelin: a transformation and shape change sensitive actin-gelling protein. J Cell Biol. 1993; 121:1065–1073. [PubMed: 8501116]

Shi J, Qian W, Yin X, Iqbal K, Grundke-Iqbal I, Gu X, Ding F, Gong CX, Liu F. Cyclic AMP-dependent protein kinase regulates the alternative splicing of tau exon 10: a mechanism involved in tau pathology of Alzheimer disease. J Biol Chem. 2011; 286:14639–14648. [PubMed: 21367856]

Smirnova E, Griparic L, Shurland DL, van der Bliek AM. Dynamin-related protein Drp1 is required for mitochondrial division in mammalian cells. Mol Biol Cell. 2001; 12:2245–2256. [PubMed: 11514614]

Spillantini MG, Murrell JR, Goedert M, Farlow MR, Klug A, Ghetti B. Mutation in the tau gene in familial multiple system tauopathy with presenile dementia. Proc Natl Acad Sci U S A. 1998; 95:7737–7741. [PubMed: 9636220]

Spradling AC, Stern D, Beaton A, Rhem EJ, Laverty T, Mozden N, Misra S, Rubin GM. The Berkeley Drosophila Genome Project gene disruption project: Single P-element insertions mutating 25% of vital Drosophila genes. Genetics. 1999; 153:135–177. [PubMed: 10471706]

Steinhilb ML, Dias-Santagata D, Fulga TA, Felch DL, Feany MB. Tau phosphorylation sites work in concert to promote neurotoxicity in vivo. Mol Biol Cell. 2007a; 18:5060–5068. [PubMed: 17928404]

Steinhilb ML, Dias-Santagata D, Mulkearns EE, Shulman JM, Biernat J, Mandelkow EM, Feany MB. S/P and T/P phosphorylation is critical for tau neurotoxicity in Drosophila. J Neurosci Res. 2007b; 85:1271–1278. [PubMed: 17335084]

Twig G, Elorza A, Molina AJ, Mohamed H, Wikstrom JD, Walzer G, Stiles L, Haigh SE, Katz S, Las G, et al. Fission and selective fusion govern mitochondrial segregation and elimination by autophagy. EMBO J. 2008; 27:433–446. [PubMed: 18200046]

Verstreken P, Ly CV, Venken KJ, Koh TW, Zhou Y, Bellen HJ. Synaptic mitochondria are critical for mobilization of reserve pool vesicles at Drosophila neuromuscular junctions. Neuron. 2005; 47:365–378. [PubMed: 16055061]

Wang X, Su B, Fujioka H, Zhu X. Dynamin-like protein 1 reduction underlies mitochondrial morphology and distribution abnormalities in fibroblasts from sporadic Alzheimer's disease patients. Am J Pathol. 2008; 173:470–482. [PubMed: 18599615]

Watanabe T, Hosoya H, Yonemura S. Regulation of myosin II dynamics by phosphorylation and dephosphorylation of its light chain in epithelial cells. Mol Biol Cell. 2007; 18:60–16.

Waterham HR, Koster J, van Roermund CW, Mooyer PA, Wanders RJ, Leonard JV. A lethal defect of mitochondrial and peroxisomal fission. N Engl J Med. 2007; 356:1736–1741. [PubMed: 17460227]

Wittmann CW, Wszolek MF, Shulman JM, Salvaterra PM, Lewis J, Hutton M, Feany MB. Tauopathy in Drosophila: Neurodegeneration Without Neurofibrillary Tangles. Science. 2001; 293:711–714. [PubMed: 11408621]

Yin HL, Stossel TP. Control of cytoplasmic actin gel-sol transformation by gelsolin, a calcium-dependent regulatory protein. Nature. 1979; 281:583–586. [PubMed: 492320]

Youle RJ, Narendra DP. Mechanisms of mitophagy. Nat Rev Mol Cell Biol. 2011; 12:9–14. [PubMed: 21179058]

Zhao DB, Cote S, Jahnig F, Haller J, Jackle H. Zipper encodes a putative integral membrane protein required for normal axon patterning during Drosophila neurogenesis. EMBO J. 1988; 7:1115–1119. [PubMed: 3402433]

Zuchner S, Mersiyanova IV, Muglia M, Bissar-Tadmouri N, Rochelle J, Dadali EL, Zappia M, Nelis E, Patitucci A, Senderek J, et al. Mutations in the mitochondrial GTPase mitofusin 2 cause Charcot-Marie-Tooth neuropathy type 2A. Nat Genet. 2004; 36:449–451. [PubMed: 15064763]

Highlights

- Tau mediates neurodegeneration through disruption of mitochondrial dynamics
- Tau expression prevents localization of the fission protein DRP1 to mitochondria
- F-actin and myosin regulate localization of DRP1 to mitochondria

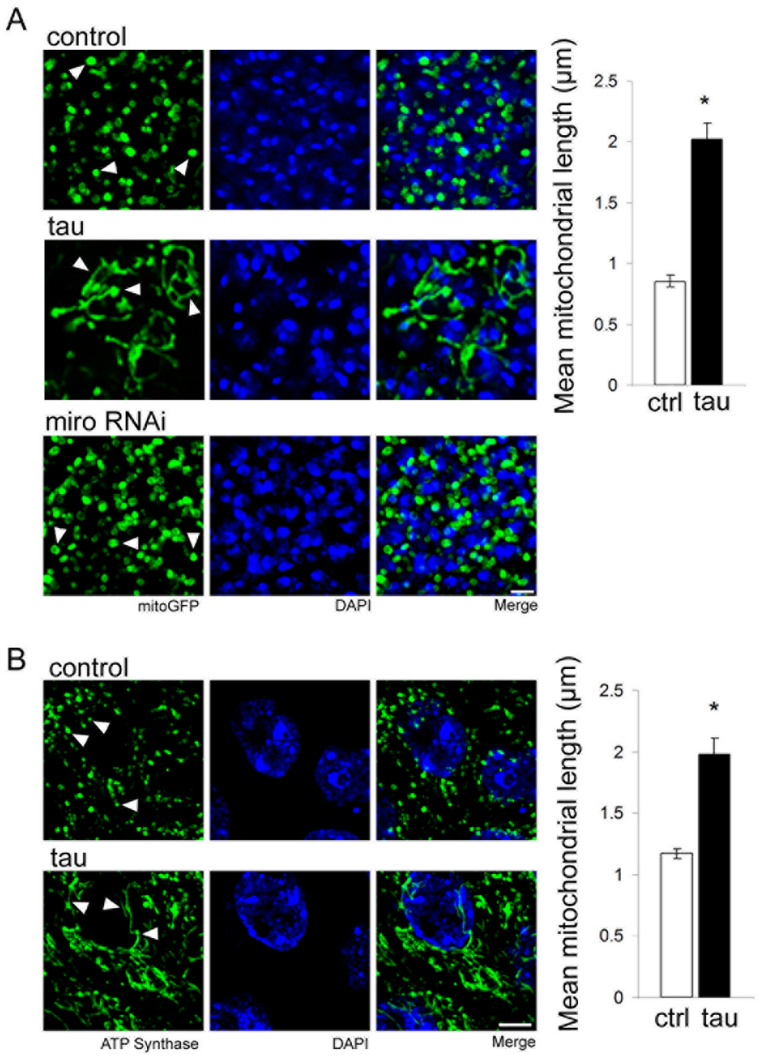

Figure 1. Tau expression promotes mitochondrial elongation in neurons in vivo

(A) Immunofluorescent staining for GFP in neurons of flies expressing mitochondrially-targeted GFP (mitoGFP) reveals normal round to modestly tubular mitochondria in control flies of the genotype *elav-GAL4/+;* UAS-mitoGFP/+ (control, arrowheads). Mitochondria in tau transgenic flies are elongated (tau, arrowheads). Reduction of miro (miro RNAi) increases the number of mitochondria in neuronal soma, but does not alter mitochondrial morphology (arrowheads). Nuclei are stained with DAPI. Scale bar is 2 μm. Quantification of mean mitochondrial length for control and tau transgenic neurons is displayed in the graph. Asterisk indicates $P < 0.01$, unpaired *t*-test, n = 6. Control (ctrl) is *elav-GAL4/+*. (B) Immunofluorescent staining for ATP synthase in CA1 hippocampal neurons of control mice demonstrates normal modestly tubular mitochondria (control, arrowheads). Mitochondria in hippocampal neurons from human tau P301L transgenic mice are elongated (tau, arrowheads). Nuclei are stained with DAPI. Scale bar is 5 μm. Quantification of mean mitochondrial length for control and tau transgenic neurons is displayed in the graph. Asterisk indicates $P < 0.01$, unpaired *t*-test, n = 3. See also Fig. S1.

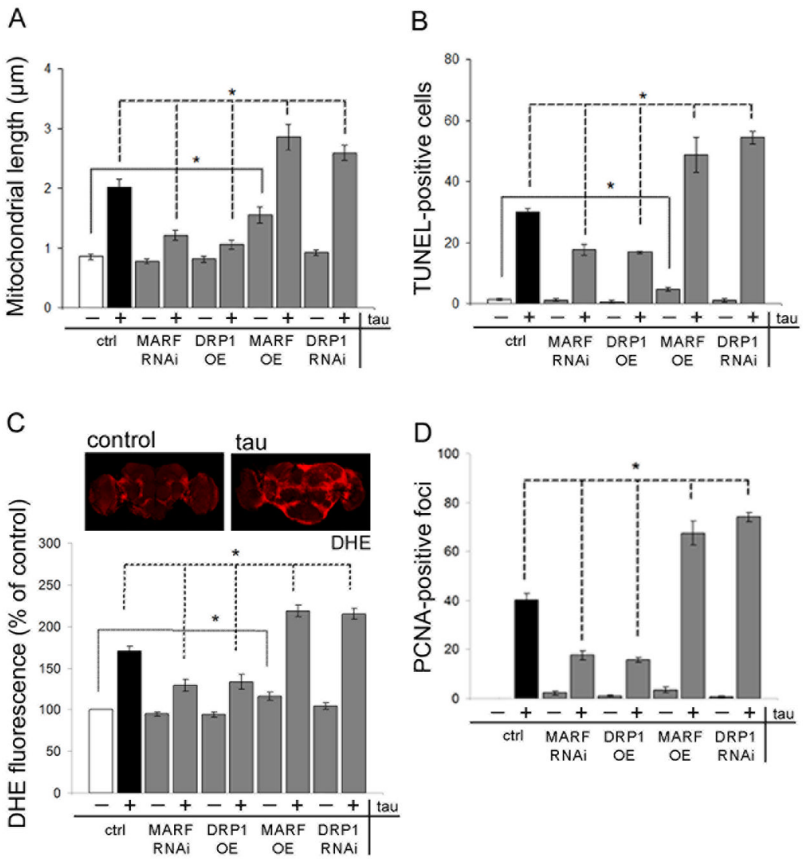

Figure 2. Genetic modification of mitochondrial dynamics influences tau toxicity

MARF is overexpressed using a *UAS-MARF* transgene (MARF OE) or reduced with transgenic RNAi (MARF RNAi). DRP1 is overexpressed using a *UAS-DRP1* transgene (DRP1 OE), or reduced with transgenic RNAi (DRP1 RNAi). Tau is expressed when indicated (tau). (A) Mitochondrial length in neurons is altered by *DRP1* or *MARF* manipulation in transgenic flies. n = 6 per genotype. Control (ctrl) is *elav-GAL4/+;*UAS-mitoGFP/+. (B) Neuronal degeneration as assayed by TUNEL staining is modified by *DRP1* or *MARF* manipulation. n = 6 per genotype. (C) Oxidative stress is evaluated by quantification of dihydroethidium (DHE) fluorescence in whole mount brains, and shows elevated levels in tau transgenic flies compared to control. Quantification of DHE fluorescence in brain shows modification following *DRP1* or *MARF* manipulation. n = 3 per genotype. (D) Cell cycle activation as measured by PCNA immunostaining is modified by *DRP1* and *MARF* manipulation. n = 6 per genotype. Asterisks indicate $P < 0.01$, one-way ANOVA with Student-Neuman-Keuls test. Control (ctrl) in (B–D) is *elav-GAL4/+*. See also Fig. S2.

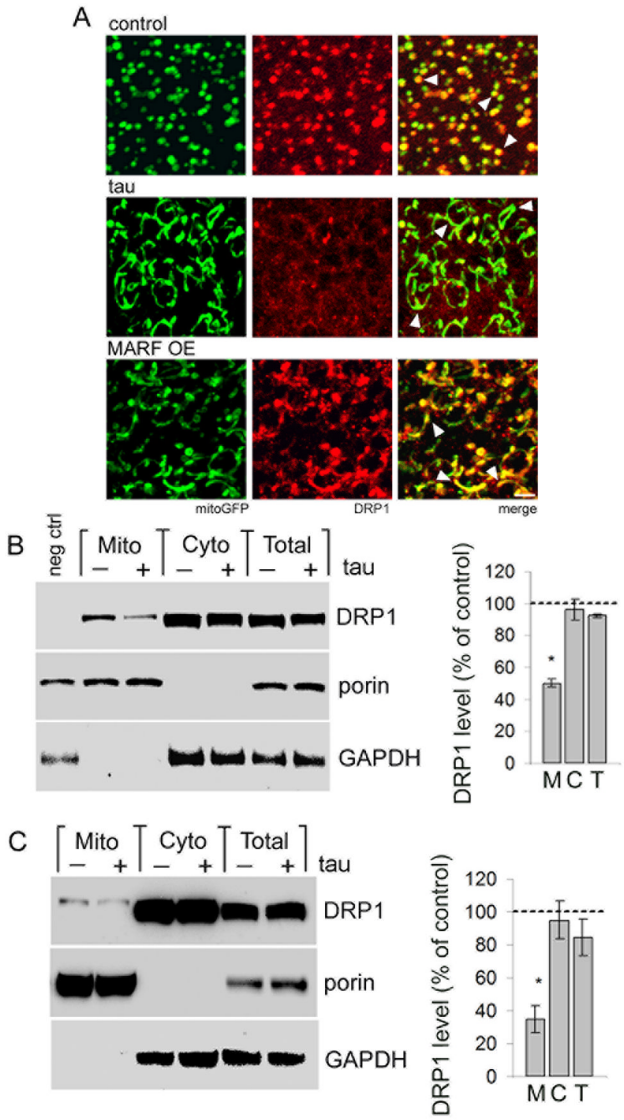

Figure 3. Tau expression blocks mitochondrial localization of DRP1

(A) Mitochondria (mitoGFP, green) and HA-tagged DRP1, detected with an antibody to HA (red), colocalize in control neurons (control, arrowheads). Mitochondria in tau transgenic neurons show markedly reduced colocalization with DRP1 (tau, arrowheads). Elongated mitochondria produced by overexpression of MARF retain the ability to recruit DRP1 (MARF OE, arrowheads). Scale bar is 2 μm. Control is *elav-GAL4/+*; UAS-mitoGFP/+; HA-DRP1/+. (B) Subcellular fractionation of fly head homogenates shows depletion of HA-DRP1, detected with an antibody to HA, from the mitochondrial fraction of tau flies (Mito, M) with equivalent levels of DRP1 in the cytoplasmic fraction (Cyto, C) or total homogenate (Total, T). Control is *elav-GAL4/+;* HA-DRP1/+, negative control (neg ctrl) is *elav-GAL4/+*. (C) Subcellular fractionation of mouse hippocampal homogenates shows reduction of mitochondrially-localized DRP1 in tau animals (Mito, M), while total (Total, T) and cytoplasmic (Cyto, C) DRP1 levels are not significantly affected. The blots in (B,C) are reprobed for porin and GAPDH to demonstrate enrichment of mitochondrial and cytoplasmic proteins in the appropriate fractions. The graphs in (B,C) show DRP1 levels as

percent of control in each fraction from tau transgenic flies or mice. Asterisks indicate $P < 0.01$, one-way ANOVA with Student-Neuman-Keuls test, n = 3. See also Fig. S3.

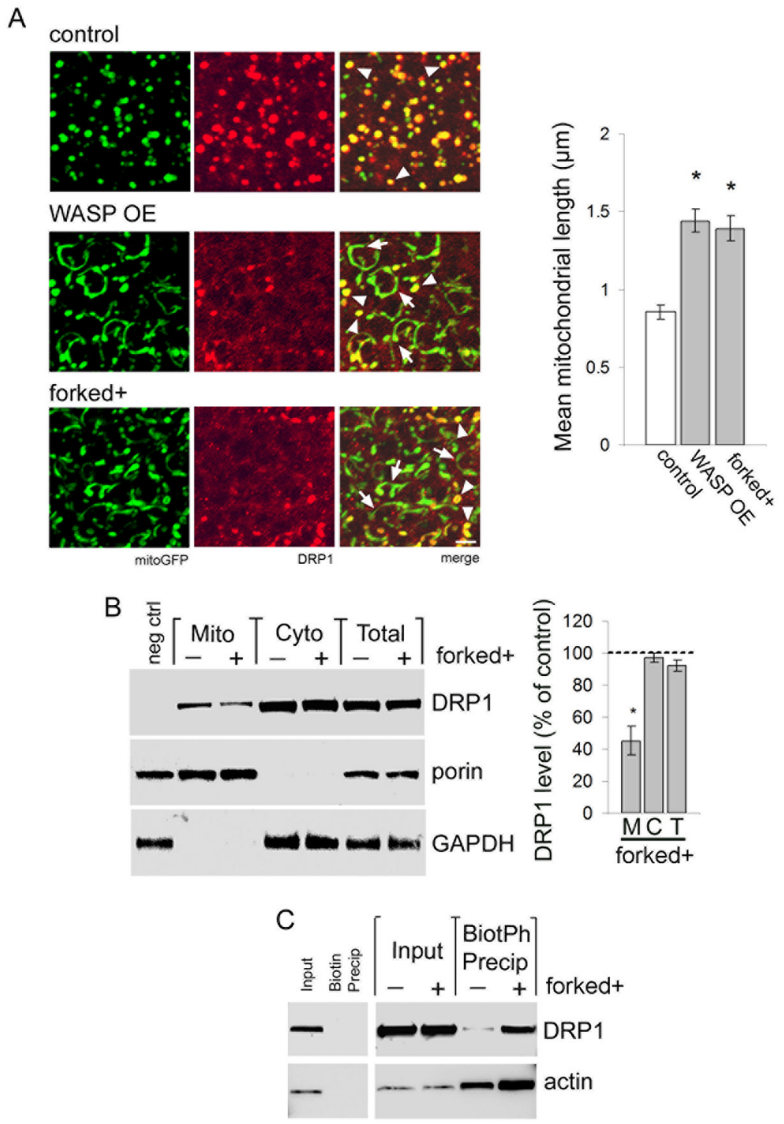

Figure 4. Actin stabilization blocks mitochondrial localization of DRP1

(A) Mitochondria (mitoGFP, green) are round to modestly tubular in control neurons and colocalize with HA-DRP1 (red, arrowheads). In flies overexpressing WASP using a *UAS-WASP* transgene (WASP OE) or forked using a genomic rescue construct (forked+) mitochondria are frequently elongated (arrows). DRP1 fails to localize to elongated mitochondria, but DRP1 colocalization is preserved in some mitochondria of normal length (arrowheads). Control is *elav-GAL4/+;* UAS-mitoGFP/+; HA-DRP1/+. Scale bar is 2 μm. Quantification of mean mitochondrial length for control, WASP OE, and forked+ is displayed in the graph. Asterisk indicates $P < 0.01$, one-way ANOVA with Student-Neuman-Keuls test. n = 6 per genotype. (B) Subcellular fractionation shows reduced HA-DRP1 in mitochondrial fractions of head homogenates from forked+ flies (Mito, M). DRP1 levels are equivalent in cytoplasmic fractions (Cyto, C) and total fractions (Total, T). The blot is reprobed for porin and GAPDH to demonstrate enrichment of mitochondrial and cytoplasmic proteins in the appropriate fractions. DRP1 level as percent of control is calculated for each fraction from forked flies (graph). Control is *elav-GAL4/+;* HA-DRP1/+, negative control (neg ctrl) is *elav-GAL4/+*. Asterisk indicates $P < 0.01$, one-way ANOVA

with Student-Neuman-Keuls test, n = 3. (C) Isolation of F-actin from control and forked+ flies by precipitation with biotinylated phalloidin (BioPh) followed by immunoblotting for actin or HA-DRP1 demonstrates a physical interaction between F-actin and DRP1, which is regulated by the stabilization state of actin. Precipitation with non-coupled biotin controls for association specificity. Control is *elav- GAL4/+;* HA-DRP1/+. n = 3. See also Fig. S4.

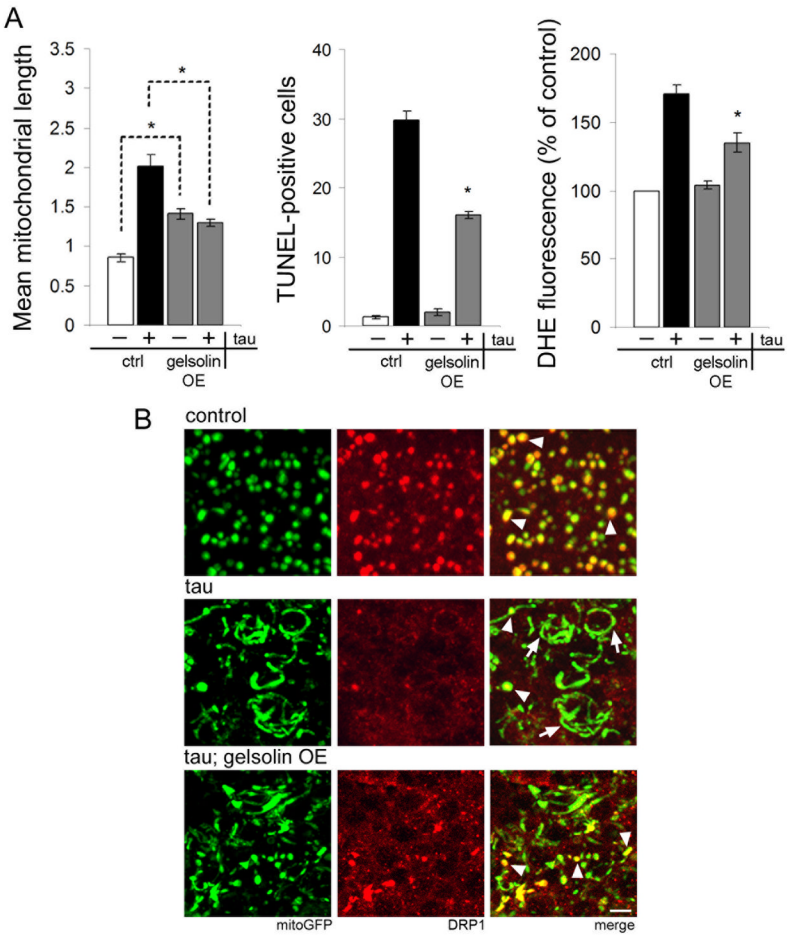

Figure 5. Reversing actin stabilization rescues tau-induced mitochondrial defects

(A) Overexpression of gelsolin using a *UAS-gelsolin* transgene (gelsolin OE) rescues mitochondrial morphology (mitochondrial length, left), neurotoxicity (TUNEL, center), and oxidative stress (DHE, right) in tau transgenic animals. Control (ctrl) is *elav-GAL4/+;* UAS-mitoGFP/+ for (left) and *elav-GAL4/+* for (center, right). Asterisk indicates $P < 0.01$, one-way ANOVA with Student-Neuman-Keuls test. n = 6 per genotype for mitochondrial length and TUNEL. n = 3 for DHE. (B) Normal mitochondria in control neurons colocalize with HA-DRP1 (control, arrowheads). Expression of tau reduces the frequency of DRP1-associated mitochondria (tau, arrowheads) in favor of elongated mitochondria lacking DRP1 (tau, arrows). Coexpression of the actin severing protein gelsolin with tau reduces mitochondrial length and restores DRP1 localization to mitochondria (tau; gelsolin OE, arrowheads). Control is *elav-GAL4/+*; UAS-mitoGFP/+; HA-DRP1/+. Scale bar is 2 μm. See also Fig. S5.

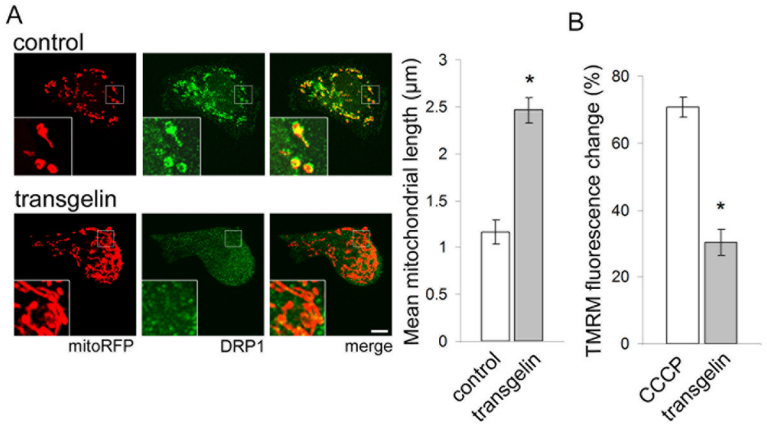

Figure 6. F-actin interacts with DRP1 to regulate mitochondrial morphology

(A) Immunofluorescence of DRP1 (green) and visualization of mitochondria with transfected mitochondrially-localized RFP (mitoRFP, red) in empty vector control shows small, round mitochondria colocalized with DRP1 (inset). Transgelin transfection inhibits association of DRP1 with mitochondria (inset), causing elongation of mitochondria and diffuse DRP1 localization. Scale bar is 10 μm. Mean mitochondrial length is quantified in the graph. (B) Mitochondrial membrane potential measured as percent change in TMRM fluorescence compared with empty vector control shows reduced membrane potential in response to CCCP depolarizing control and transgelin transfection. Asterisk indicates $P < 0.01$, unpaired *t*-test. n = 6. See also Fig. S6.

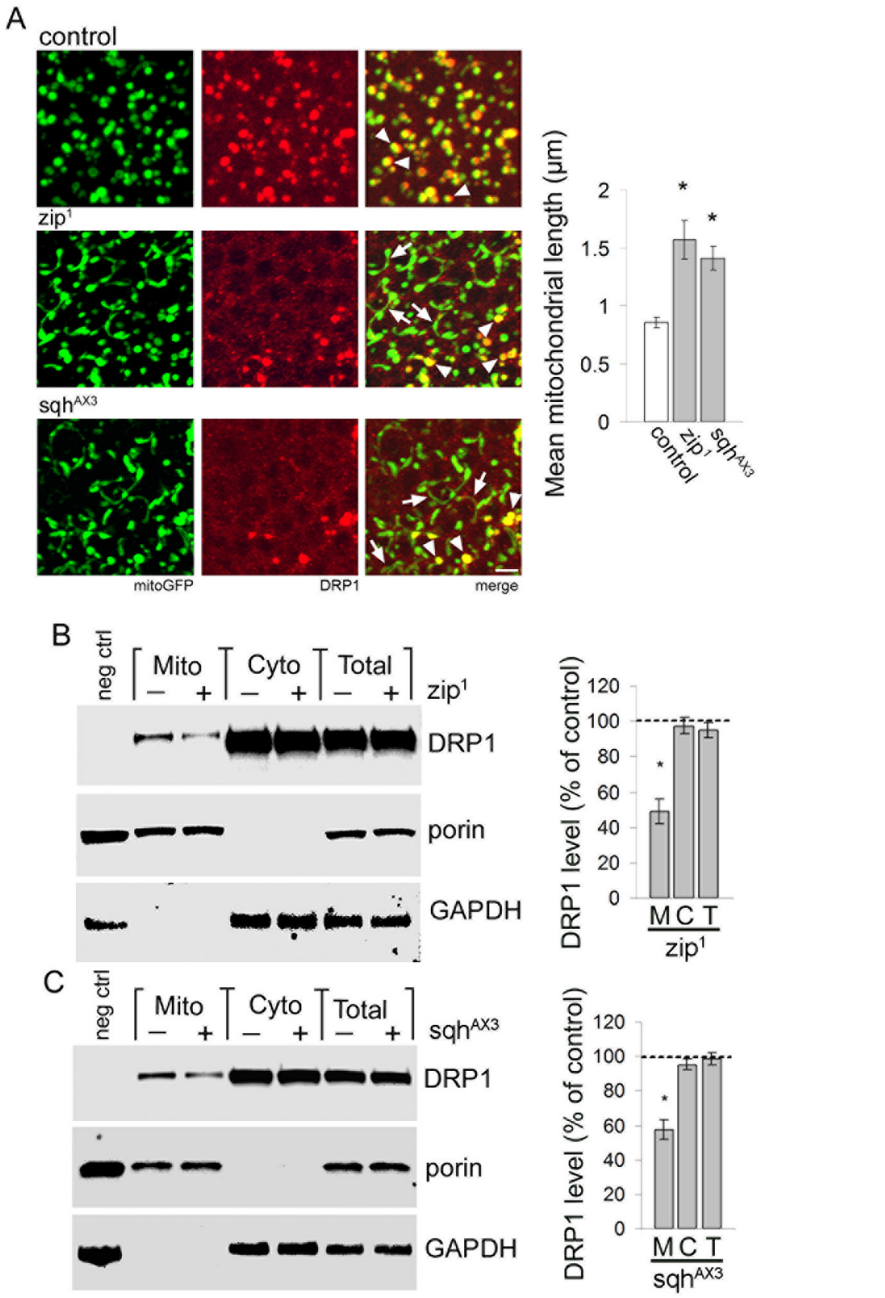

Figure 7. Myosin II facilitates colocalization of DRP1 with mitochondria

(A) In control *Drosophila* neurons mitochondria (green) are short and colocalize with HA-DRP1 (red, arrowheads). Neurons from flies heterozygous for *zip*^{1} or *sqh*^{AX3}, loss-of-function alleles of the *Drosophila* homologs of mammalian myosin II heavy chain and regulatory light chain, respectively, have elongated neuronal mitochondria that do not associate with DRP1 (*zip*^{1} and *sqh*^{AX3}, arrows). Normal round to modestly tubular mitochondria often retain DRP1 (*zip*^{1} and *sqh*^{AX3}, arrowheads). Control is *elav-GAL4/+;* UAS-mitoGFP/+; HA-DRP1/+. Scale bar is 2 μm. Mean mitochondrial length is quantified in the graph. Asterisk indicates $P < 0.01$, one-way ANOVA with Student-Neuman-Keuls test. n = 6. (B–C) Subcellular fractionation shows reduced HA-DRP1 in mitochondrial fractions of head homogenates from flies with reduced zip (B) or sqh (C) levels (*zip*^{1} and

sqh^{AX3}, Mito, M). DRP1 levels are equivalent in cytoplasmic fractions (Cyto, C) and total fractions (Total, T). The blot is reprobed for porin and GAPDH to demonstrate enrichment of mitochondrial and cytoplasmic proteins in the appropriate fractions. DRP1 level as percent of control is calculated for each fraction (graph). Control is *elav-GAL4/+;* HA-DRP1/+, negative control (neg ctrl) is *elav-GAL4/+,* HA-DRP1/+, *zip*^{1} is *elav-GAL4/+; zip*^{1}*/+*; HA-DRP1/+, *sqh*^{AX3} is *elav-GAL4/sqh*^{AX3}; HA-DRP1/+. Asterisk indicates $P < 0.01$, one-way ANOVA with Student-Neuman-Keuls test, n = 3. See also Fig. S7.

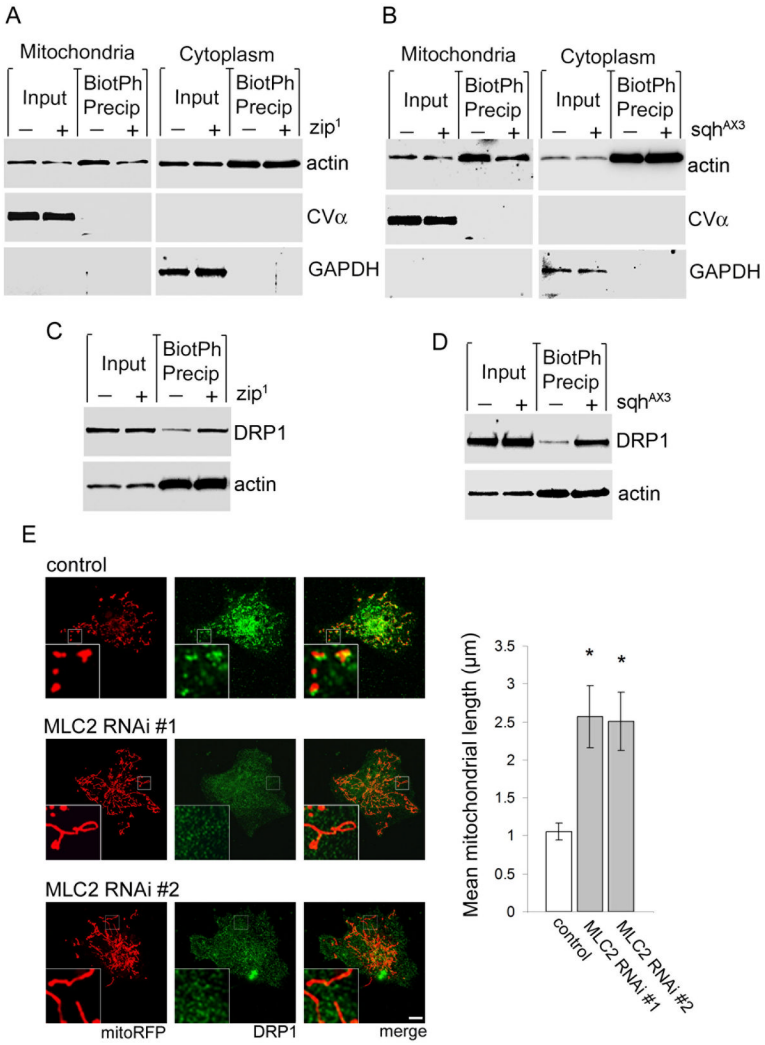

Figure 8. Myosin II links mitochonria with F-actin

(A–B) Precipitation of F-actin with biotinylated phalloidin from isolated mitochondrial fractions of heterozygous *zip*^{1} (A, Mitochondria) and *sqh*^{AX3} (B, Mitochondria) fly heads followed by immunoblotting for actin reveals a depletion in mitochondria-associated F-actin compared to control (BiotPh Precip). The depletion is also apparent in total actin (Input). Cytoplasmic F- actin and total actin levels are equivalent between control and both *zip*^{1} and *sqh*^{AX3} flies (Cytoplasm). The blots are reprobed for Complex Vα and GAPDH to demonstrate enrichment of mitochondrial and cytoplasmic proteins in the appropriate fractions. n = 3. (C–D) Coprecipitation of DRP1 and F-actin using biotinylated phalloidin in total head homogenate from heterozygous *zip*^{1} (C) and *sqh*^{AX3} (D) flies reveals no change in total actin (Input) or F-actin (BiotPh Precip) levels compared to control. However, both *zip*^{1} and *sqh*^{AX3} increase the level of DRP1 coprecipitating with F-actin. n = 3. In (A–D) control is *elav-GAL4/+;* HA-DRP1/+, *zip*^{1} is *elav-GAL4/+; zip*^{1}*/+*; HA-DRP1/+, *sqh*^{AX3} is *elav-GAL4/sqh*^{AX3}; HA-DRP1/+. (E) In control Cos-1 cells transfected with mitoRFP and control siRNA mitochondria (red) are round or modestly tubular and associated with endogenous DRP1 (green, inset). Transfection of either of two siRNAs targeting non-overlapping sequences in MLC2 results in mitochondrial elongation and inhibits localization of DRP1 to mitochondria (inset). Mean mitochondrial length is quantified in the graph.

Asterisk indicates $P < 0.01$, one-way ANOVA with Student-Neuman-Keuls test, n = 6. See also Fig. S8.